



ORIGINAL ARTICLE

Green formulation, chemical characterization, and antioxidant, cytotoxicity, and anti-human cervical cancer effects of vanadium nanoparticles: A pre-clinical study



Yunping Zhang^a, Xin Zhang^b, Lan Zhang^{c,*}, Abdullah A. Alarfaj^d,
Abdurahman H. Hirad^d, Ahmed E. Alsabri^d

^a Central Sterile Supply Department, The Second Affiliated Hospital of Xi'an Jiaotong University, Xi'an 710004, China

^b Department of Obstetrics and Gynecology, The Second Affiliated Hospital of Xi'an Jiaotong University, Xi'an 710004, China

^c Department of Endocrinology, The Second Affiliated Hospital of Air Force Medical University, Xi'an 710038, China

^d Department of Botany and Microbiology, College of Science, King Saud University, P.O. Box 2455, Riyadh 11451, Saudi Arabia

Received 10 February 2021; accepted 28 March 2021

Available online 17 April 2021

KEYWORDS

Vanadium nanoparticles;
Calendula officinalis leaf;
Chemotherapeutic drug;
Human cervical cancer

Abstract In this study, V_2O_5 nanoparticles were synthesized in an aqueous medium using *Calendula officinalis* extract as stabilizing and reducing agents. The synthesized nanoparticles (VNPs@*C.officinalis*) were characterized using different techniques including UV-Vis. and FT-IR Spectroscopy, X-ray Diffraction (XRD), Scanning Electron Microscopy (SEM), and Energy Dispersive X-ray Spectrometry (EDS). According to the XRD analysis, 28.83 nm was measured for VNPs@*C.officinalis* crystal size. SEM images exhibited a uniform spherical morphology in size of 38.14 nm for the biosynthesized nanoparticles. To survey the cytotoxicity and anti-human cervical cancer effects of *C. officinalis* aqueous extract and vanadium nanoparticles, MTT assay was used on C-33 A [c-33a], SiHa, Ca Ski, DoTe2 4510, HT-3, and LM-MEL-41 cell lines. The IC50 of the vanadium nanoparticles were 237, 259, 226, 409, 335, and 192 $\mu\text{g}/\text{mL}$ against C-33 A [c-33a], SiHa, Ca Ski, DoTe2 4510, HT-3, and LM-MEL-41 cell lines, respectively. To survey the antioxidant properties of *Calendula officinalis* aqueous extract and vanadium nanoparticles, the DPPH test was used. The vanadium nanoparticles inhibited half of the DPPH molecules in a concentration of 125 $\mu\text{g}/\text{mL}$. As mentioned, the vanadium nanoparticles had significant antioxidant and anti-human cervical cancer effects.

© 2021 Published by Elsevier B.V. on behalf of King Saud University. This is an open access article under the CC BY-NC-ND license (<http://creativecommons.org/licenses/by-nc-nd/4.0/>).

* Corresponding author.

E-mail address: zhanglan206@sina.com (L. Zhang).

Peer review under responsibility of King Saud University.



1. Introduction

Uterine is one part of the genital system that its normal function is necessary for the routine activities of the body. The major disorders that influence the normal action of uterine are cervical cancers, uterine cancers, endometriosis, uterine fibroids, metritis, and uterine infections (Clarke et al., 2018). Cervical cancer is a cancer of the uterus lining. Cervical cancer is the main cancer in both developing and developed countries (Clarke et al., 2018). The main risk factors of cervical cancer are increasing age, late menopause, use of tamoxifen, obesity, high levels of estrogen, breast cancer, never having had a child, and diabetes mellitus. Many mutations such as ARID1A, CTNNB1, FGFR2, KRAS, PIK3R1, TP53, PTEN, MLH1, RASSF1A, SPRY2, PPP2R1A, CDH1, CDKN2A, PIK3CA, PIK3R1, STK15, CCNE1, ERBB2, and CCND1 arise the rate of cervical cancer (Burke et al., 2014). The signs of cervical cancer are infertility, vaginal bleeding, uterine bleeding, pelvic pain, pain during sexual intercourse, and pain with urination (Burke et al., 2014; Clarke et al., 2018). Cervical screening tests, pap smear, a transvaginal ultrasound, endometrial biopsy, CT scan, and hysteroscopy are used to diagnose cervical cancer (Murali et al., 2014).

To treat cervical cancer, chemotherapy, radiation therapy, and immunotherapy are used. The major anti-endometrial cancer chemotherapeutic materials are carboplatin, paclitaxel, docetaxel, doxorubicin, and cisplatin (Guillotin and Martin, 2014). Due to severe side effects of the chemotherapeutic drugs and supplements, the formulation of the chemotherapeutic drugs from metallic nanoparticles such as vanadium nanoparticles are the research priority of pharmacology, oncology, and organic chemistry researchers (Arunachalam et al., 2013; Ghashghaii et al., 2017; Goorani et al., 2019; Abdole et al., 2020; Jalalvand et al., 2019; Moradi et al., 2019; Prasad et al., 2018; Rashidi et al., 2018; Raut et al., 2010; Sherkatolabbasieh et al., 2017; Sintubin et al., 2009). Nowadays, nanotechnology has been developed in several ways due to its wide range of applications. The surface area to volume ratio of nanoparticles makes them potent agents in biological aspects (Khan et al., 2019). Nanomaterials have better physicochemical features than their counterparts, some of these features are as follows: optical, toxicity, color, prevalence, solubility, strength, thermodynamics, magnetic, etc. Metallic nanoparticles with various properties and a wide range of activity have been well known (Fahimmunisha et al., 2020).

The present time's biological methods that are eco-friendly, non-toxic, and cost-effective have been developed for the synthesis of nanoparticles instead of the previous methods (Ghashghaii et al., 2017; Sherkatolabbasieh et al., 2017). Biogenic synthesis of nanoparticles from the salts of metal ions is done under 'green' condition, to attain this purpose used reducing factors, an eco-friendly solvent system, and eco-friendly stabilizing (Raut et al., 2010). Many pharmaceutical plants and microorganisms can be used for formulating nanoparticles, the reduction process of metal ions due to special factors found in organisms that an important principle in the biogenesis of nanoparticles (Prasad et al., 2018). Since the decade from 1900 to 1909, the application of plant extracts for the reduction of metal ions has been a known method. Due to the lack of understanding of reducing factors in the last

30 years, the interest in researching them has increased (Arunachalam et al., 2013; Sintubin et al., 2009). Studies have recently reported that pharmaceuticals plants green synthesized metal nanoparticles have efficient anti-cancer features. Metallic nanoparticles have received special attention in the field of medicine. Recently some investigations have shown that some nanoparticles have remedial features and are an excellent alternative to some drugs such as antibacterial, antifungal, etc (Abdoli et al., 2020; Jalalvand et al., 2019).

In the recent years, the applications of vanadium oxide with nanostructure has been growing; due to its chemical and physical properties. The vanadium oxide NPs is used as catalyst, sensor in the synthetic, electrochemical or optical field. Vanadium NPs also shows applications in biological and medical science (Aliyu et al., 2017; Deepika et al., 2020; Kang et al., 2014; Karthik et al., 2020). A review on literature reveals that different methods such as ultrasonication route, vacuum evaporation, electrodeposition, hydrothermal, and sol-gel have been reported to synthesis nanoparticles of vanadium oxide (Karthik et al., 2020; Talavera et al., 2013). Most of these procedures are classified in non-friendly environmental methods. However, a few studies have reported the green synthesis of vanadium oxide NPs. In this research, we focus on the biosynthesis of vanadium nanoparticles using aqueous extract of *Calendula officinalis* and evaluation of cytotoxicity, antioxidant, and anti-human cervical cancer effects against C-33 A [c-33a], SiHa, Ca Ski, DoTc2 4510, HT-3, and LM-MEL-41 cell lines for the first time.

2. Material and methods

2.1. Material

Bovine serum, Dulbecco's Modified Eagle Medium (DMEM), antimycotic antibiotic solution, 2,2-diphenyl-1-picrylhydrazil (DPPH), dimethyl sulfoxide (DMSO), decamplmaneh fetal, 4-(Dimethylamino) benzaldehyde, hydrolyzate, Ehrlich solution, and borax-sulfuric acid mixture, Dulbazolic mixture Modified Eagle Medium (DMED), all were afforded from the US Sigma-Aldrich company.

2.2. Preparation and synthesis of vanadium nanoparticles containing *Calendula officinalis*

To obtain the aqueous extract of the plant, first the plant parts was rinsed by tap water and then dried in shadow. Next, 100 gr of the dried branches of the *Calendula officinalis* leaves were poured in a container containing 1000 ml boiled water, and the container lid was tightly closed for 4 h. Then, the container's content was filtered, and the remaining liquid was placed on a bain-marie to evaporate. Finally, a tar-like material was obtained, which was powdered by a freeze dryer.

The biosynthesis of VNPs@*C.officinalis* was carried out according to the previous study (Prasad et al., 2018). A 25 ml of aqueous extract solution (10 mg/mL) was added to 25 ml of sodium metavenadatein at the concentration of 0.02 M (Deionized water was used for all steps of this section). The mixture was stirred for 90 min at room temperature. The formed yellow-orange precipitate was triplet washed with water and centrifuged at 12000 rpm for 15 min subsequently.

The residue was dried and kept in a vial for the chemical characterization and evaluation of its biological activity.

2.3. Chemical characterization techniques

To characterize and measure of different parameters of the biosynthesized VNP@*C.officinalis*, various techniques, including UV-Vis. and FT-IR spectroscopy, XRD, SEM, and EDS techniques, were applied. The UV-Vis. spectra were obtained using Cray 50 UV-Vis. spectrophotometer (200–800 nm); The FT-IR spectra were recorded using a Shimadzu FT-IR 8400 in the range of 400–4000 cm^{-1} (KBr disc); MIRA3TESCAN-XMU was used to report the FE-SEM Images and EDS result. The XRD pattern of VNPs was recorded in the 2θ range of 20–80° by a GNR EXPLORER instrument (voltage of 40 kV, a current of 30 mA, and $\text{Cu-K}\alpha$ radiation 1.5406 Å).

2.4. Anti-human cervical cancer properties of vanadium nanoparticles containing *Calendula officinalis*

The MTT assay is a procedure of colorimetric based on reducing and breaking of yellow tetrazolium crystals by the enzyme succinate dehydrogenase to form insoluble purple crystals. In this method, unlike other methods, the steps of washing and collecting cells, which often cause the loss of a number of cells and increase the work error, have been eliminated and all test steps from the beginning of cell culture to reading the results with a photometer are performed on a microplate, so the repeatability, accuracy and sensitivity of the test are high (Mao et al., 2016; Namvar et al., 2014; Sankar et al., 2014; Tahvilian et al., 2019; You et al., 2012). If the test is performed on cells attached to the plate, an appropriate number of cells (about 2,000 cells) must first be cultured in each of the wells. Then we select the control and test wells and add the appropriate amount of mitogen or drug to the test wells and place the plate in the incubator for the required time so that the desired substance affects the cells (Mao et al., 2016; Namvar et al., 2014; Sankar et al., 2014; Tahvilian et al., 2019; You et al., 2012). At the end of the incubation time, discard the supernatant and add 200 μl of culture medium containing half an mg/ml of MTT solution to each well and put it again in a carbon dioxide incubator for 2 to 4 h at 37 °C. During incubation, MTT is regenerated by one of the enzymes of the mitochondrial respiratory cycle i.e., succinate dehydrogenase. The regeneration and breakage of this ring produce purple-blue crystals of formazan that are easily detectable under a microscope (Mao et al., 2016; Namvar et al., 2014; Sankar et al., 2014; Tahvilian et al., 2019; You et al., 2012). At the end, the optical absorption of the resulting solution can be read at 570 nm and the cells number can be calculated using a standard curve. For each cell line, there is a linear relationship between the number of cells and the light absorption of the final solution. Therefore, to examine each cell type, a standard curve related to the same cell line must be drawn and used (Mao et al., 2016; Namvar et al., 2014; Sankar et al., 2014; Tahvilian et al., 2019; You et al., 2012).

In this research, we used the following cell lines to evaluating anti-human cervical cancer and cytotoxicity effects of vanadium nanoparticles using an MTT method.

(a) Human cervical cancer cell lines:

- C-33 A [c-33a].
- SiHa.
- Ca Ski.
- DoTc2 4510.
- HT-3.
- LM-MEL-41

(b) Normal cell line:

- HUVEC.

15 ml of RPMI 1640 medium containing 10% FSC (10 mg/ml penicillin and 100 mg/ml streptomycin) in a culture flask, placed in a CO_2 incubator for 2 h to equilibrate the medium. Under safe conditions (using insulated gloves and goggles) the frozen cell vial was removed from the nitrogen storage tank. To avoid the possibility of explosion of the vial (due to the possible entry of liquid nitrogen into the vial), loosen the lid, after disinfecting the outer surface of the vial with 70% alcohol, under the hood to remove nitrogen gas. Close the vial lid again and immediately melt it in a pan at 37° C. The melting process should be completed in about 1 min and the cells should be avoided from overheating. The medium was added dropwise to the vial and then its contents were taken out and centrifuged with the medium in 15 cc sterile test tubes. After centrifugation, the supernatant was removed and the cells were suspended again in the medium and transferred to a pre-prepared flask containing the medium and FBS and incubated (Arunachalam et al., 2013).

Cell line used in RPMI 1640 medium containing penicillin (100 IU/ML), streptomycin (100 IU/ML), glutamine (2 mmol) and 10% fetal bovine serum (FBS). They were incubated at 37 °C and in an atmosphere containing 0.5 CO_2 . Cells began to grow in 75 cm^2 T-flasks in 15 ml medium with an initial number of $1-2 \times 10^6$ cells. After three days and covering the flask bed with the cell, the adhesive layer to the bottom of the flask was separated enzymatically using trypsin-verseon and transferred to a sterile test tube for 10 min at 1200 rpm. The cells were then suspended in a fresh culture medium with the help of a Pasteur pipette and the suspension was poured into 100-well plate flat wells (for cell culture) using an 8-channel sampler of 100 μl . One column of wells was kept cell-free and as a plank containing only culture medium. In another column, it was considered to contain culture medium and healthy cells and in other columns, it was considered to contain culture medium and cell line cells. One of these columns, which contained culture medium and cells and did not contain vanadium nanoparticles, was considered as a control (Arunachalam et al., 2013).

The plates were incubated in the incubator for 24 h to return the cells to normal from the stress of trypsinization. After this time, suitable dilutions of the prepared vanadium nanoparticles (0–1000 $\mu\text{l}/\text{ml}$) and 100 μl of each dilution were added columnar to the plate wells (Thus, the final concentration of the studied compound in the wells was halved. Therefore, the concentrations were prepared twice as much to reach the final concentration after being added to the well). The cells were incubated for 37 h at 37 °C and 5% CO_2 in the atmosphere. After 72 h, 20 μl of MTT solution (5 mg/ml) was added to each well. The plates were incubated

for 3 to 4 h and then the residue was removed and 100 μl of DMSO was added to each well to dissolve the resulting formazan. After 10 min, using shaking the plates, the optical absorption of Formazan at 570 nm was read using a plate reader. Wells containing cells without vanadium nanoparticles were considered as control and the optical density of wells without cells and only culture medium were considered as blank. The percentage of cell viability was calculated using the following formula (Arunachalam et al., 2013):

$$\text{Cell viability}(\%) = \frac{\text{Sample } A}{\text{Control } A} \times 100$$

The closer is the obtained value to the IC50 of vanadium nanoparticles, the stronger is the cell viability activity of the material. The graph of the IC50 of the vanadium nanoparticles was produced by drawing the percent inhibition curve versus the vanadium nanoparticles concentration. First, three stock samples with variable concentrations (0–1000 $\mu\text{g}/\text{mL}$) of vanadium nanoparticles were prepared. Then, a serial dilution was prepared from each sample, and IC50 of the above samples was measured separately, following which their mean was calculated (Arunachalam et al., 2013).

2.5. Antioxidant activities of vanadium nanoparticles containing *Calendula officinalis*

Analysis of antioxidant capacity by the DPPH radical method is a well-known test for measuring the antioxidant power of various compounds. The basis of this method is based on the reduction of free radical DPPH by antioxidants in the absence of other free radicals in the environment. A compound is generally compared to a known antioxidant compound such as Butylated Hydroxytoluene (BHT). Analysis of antioxidant capacity by the DPPH method is a test that has received much attention in the fields of food, pharmaceuticals and biotechnology and is used to develop and introduce new antioxidants. The basis of this method is based on the reduction of free radical DPPH by antioxidants in the absence of other free radicals in the environment, which results in color in the environment whose intensity can be measured by spectroscopy. DPPH is a stable free radical that has an unpaired electron on one of the nitrogen bridge atoms. Radical inhibition of DPPH is the basis for assessing antioxidant capacity (Shaneza 'Aman et al., 2018):



DPPH is a stable radical whose methanolic solution has a purple color that shows the highest light absorption at 519–595 nm. The basis of this method is that the DPPH radical acts as an electron acceptor of a donor molecule such as an antioxidant, thus converting DPPH to DPPH2. In this case, the purple color of the environment turns yellow, so the absorption intensity decreases to 595 nm. Antioxidant properties can be determined by measuring the decrease in adsorption intensity by spectroscopy (Shaneza 'Aman et al., 2018).

In the present study to measure the antioxidant properties of the vanadium nanoparticles, 2 ml of DPPH (100 μM) dissolved in methanol with 2 ml of the vanadium nanoparticles at the concentrations of $\mu\text{g}/\text{ml}$. The resulting mixture was placed at 25 $^\circ\text{C}$ for 30 min. Then the samples absorbance was measured at 520 nm by spectrophotometer (Spectramax

Gemini XS; Molecular Devices, Sunnyvale, CA) and the amount of antioxidant effect was determined by the below formula (Shaneza 'Aman et al., 2018):

$$\% \text{ Inhibition} = [(A_{\text{blank}} - A_{\text{blank}}) / A_{\text{blank}}] \times 100$$

The blank sample consisted of a mixture of 2 ml of vanadium nanoparticles and 2 ml of methanol and a sample containing 2 ml of DPPH and 2 ml of vanadium nanoparticles with the concentrations used was considered as the negative control. BHT was also used as a positive control. Calculating the 50% inhibition error (IC50) is an excellent way to compare drug activity that dose in which 50% of the final activity of the drug occurs is the criterion for measurement and comparison. In this test, the amount of IC50 for different repetitions of the test was also calculated and is compared with IC50 of BHT molecule, which is an indicator of antioxidant activity. The closer IC50 is to BHT, the stronger the antioxidant activity. In the following experiments, the inhibition concentration of 50% of the vanadium nanoparticles was calculated by plotting the inhibition percentage curve against the vanadium nanoparticles concentration. In the next step, a serial dilution was prepared from each sample and 50% inhibition concentration of three separate samples was measured and its mean was calculated. All experiments were performed three times (Shaneza 'Aman et al., 2018).

2.6. Statistical analysis

The data were gathered and given into the "SPSS-24" a computer software program and was analyzed by "one-way ANOVA", and then the Duncan posthoc test ($p \leq 0.01$).

3. Results and discussion

In this experiment, we formulated vanadium nanoparticles by using *Calendula officinalis* leaf aqueous extract. Furthermore, in *in vitro* condition, we evaluated the anti-human cervical cancer activities of vanadium nanoparticles (0–1000 $\mu\text{g}/\text{mL}$) against common human cervical cancer cell lines i.e.C-33 A [c-33a], SiHa, Ca Ski, DoTe2 4510, HT-3, and LM-MEL-41.

3.1. Characterization of vanadium nanoparticles

3.1.1. FT-IR analysis

The method of FT-IR spectroscopy is used for detecting unknown substances, determining the quality or uniformity of the sample, determining the amount of ingredients in a mixture, identify mixtures of organic and inorganic compounds provided they are both solid or liquid, thin layer analysis, analysis of adhesives, coatings and adhesive enhancers or binders, identification of polymers and polymer mixtures, analysis of solvents, cleaners and detergents unknown, percentage of decomposition or non-polymerization of polymers and paints due to heat, UV or other factors, determination of the degree of crystallization in polymers, and analysis of resins, composite materials and metal nanoparticles (Kang et al., 2014; Karthik et al., 2020).

In FT-IR spectra of metal oxides, the vibration band for metal–oxygen bond usually appears in 400 to 700 cm^{-1} . Fig. 1 presents the FT-IR spectra of VNPs and the plant extract. As it can be seen, the both FT-IR spectra are closed

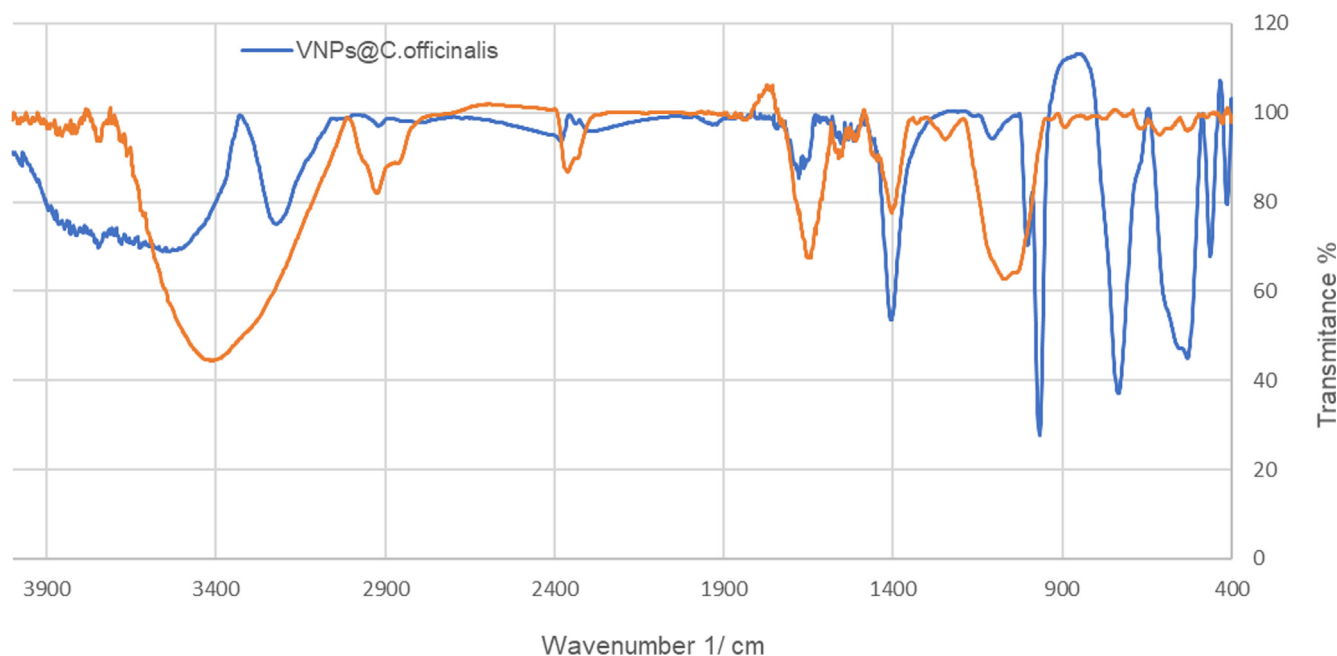


Fig. 1 FT-IR spectrum of biosynthesized VNP@*C.officinalis* and *C. officinalis* extract.

together that confirm the green synthesis of VNPs using *C. officinalis* extract. The peaks at 459, 541, and 740 cm^{-1} attributes to the bending vibration of V-O or V-O-V. These peaks for vanadium oxide nanoparticles have been reported previously with a small difference in the wavenumber (Kang et al., 2014; Karthik et al., 2020). FT-IR technique is a reliable method to evaluate the plant secondary metabolites as the capping and reducing agents of sodium metavanadate precursor to VNPs. The presence of different-IR bands correlates to the presence of various functional groups in *C. officinalis* extract. For example, peaks in 3417 and 2925 cm^{-1} related to O-H and aliphatic C-H stretching; the peaks at a range of 1471 to 1662 cm^{-1} correspond to C = C and C = O stretching, and peak at 1096 cm^{-1} could be ascribed to -C-O stretching. These peaks can be considered for the presence of various compounds in the plant extract such as phenolic, flavonoid, saponins, quinones, terpenoids which have been reported previously (de Oliveira Carvalho et al., 2018; Długosz et al., 2018; Verma et al., 2018). In biosynthetic of metallic nanoparticles, the secondary metabolite of plant extracts, as reducing, stabilizing, and dispersing agents usually bind to NPs over their functional groups of hydroxyl and carbonyl (Ghidan et al., 2016).

3.1.2. XRD analysis

X-ray diffraction is applied to investigate the crystalline materials structures. The X-ray region in the electromagnetic spectrum is in the range between the beam and the ultraviolet. Using this spectral region, information can be obtained about the structure, material, and quantification of the elements. Therefore, x-ray diffraction methods have many applications in decomposition chemistry. For a pure substance, the X-ray diffraction pattern is the same as for a fingerprint. So far, the diffraction pattern of more than 75,000 inorganic and organic compounds has been collected (Karthik et al., 2020). Using this database and with the help of the search and match-

ing method, the composition of each material can be determined. X-ray diffraction is used in characterizing the crystal structure of materials, including measuring the average distances between layers and atomic series, determining the position of a single crystal or grain and the composition of atoms ..., examining the crystal structure of unknown materials, determining structural characteristics including lattice parameter, size and shape (Karthik et al., 2020). In the XRD method, the size of the crystals can be determined in certain conditions using the Scherer equation. It is also used to detect crystal phases and their position and to measure thickness, thin films and multilayers. Although X-ray diffraction has many applications, its most important application is in estimating the size of crystals in crystal structures (Karthik et al., 2020).

Fig. 2 shows the XRD pattern of VNP@*C.officinalis*. The result, same to FT-IR spectra, approves the synthesis of vana-

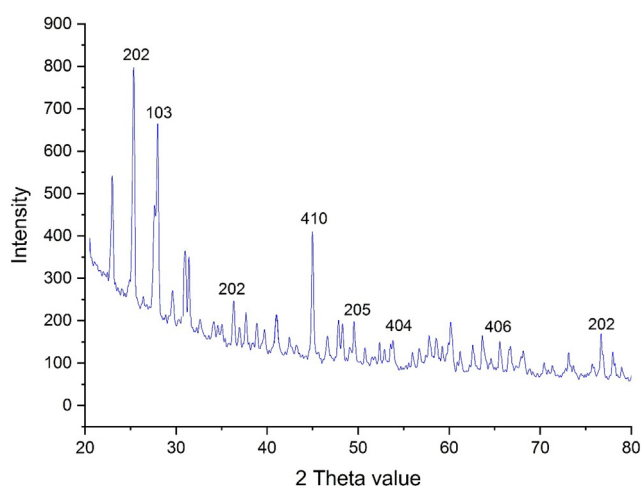


Fig. 2 XRD Pattern of VNP@*C.officinalis*.

dium oxide. Eight peaks at 2θ values of 25.27, 27.95, 37.63, 44.94, 49.49, 53.56, 66.71, and 76.71 are indexed as (202), (103), (202), (410), (205), (404), (406), and (202) planes. These peaks are matched as well as to those of standard database JCPDS no: 85–2422 for vanadium oxide. The peaks at different degrees are also reported previously (Karthik et al., 2020). The average crystal size of VNPs@*C.officinalis* was calculated using X-ray diffraction according to the Scherrer equation

$$D = \frac{k\lambda}{\beta\cos\theta}$$

The vanadium oxide nanoparticles had an average crystal size of 28.83 nm.

3.1.3. SEM and TEM analysis

Today, SEM is used not only in materials science, chemistry and physics, but also in many fields such as medical and biological sciences. The high resolution of SEM makes it one of the most-powerful and comprehensive tools for examining and analyzing a wide range of microstructure characteristics of samples at the nanometer to micrometer scale. Using the above technique, we can determine how the particles are placed from each other, their morphology and size (Ahmeda et al., 2020; Baghayeri et al., 2018).

SEM and TEM images of VNPs@*C.officinalis* are shown in Fig. 3 (a-c). The both techniques depict a spherical morphology for the VNPs. This morphology for biosynthesized VNPs

has been reported previously (Aliyu et al., 2017; Karthik et al., 2020). The figure also confirms the uniformity, well dispersed, and homogeneous of the VNPs. Similar to the other metallic nanoparticles, which have synthesized using green chemistry approaches, a propensity to aggregate is observed for VNPs@*C.officinalis*. This property has been reported by others for VNPs, Zn NPs, SnNPs, AgNPs, and TiNPs (Ahmeda et al., 2020; Baghayeri et al., 2018; Karthik et al., 2020; Mahdavi et al., 2020; Mahdavi et al., 2019; Seydi et al., 2019; Sintubin et al., 2009). The average size of diameter for VNPs was 38.14 nm by SEM images and according to TEM image most of nanoparticles were less than 100 nm. In our review of literature, different sizes have been reported for the biosynthesized V_2O_5 NPs. According to the previous studies, VNPs has been synthesized in various value for the particle size from 10 to 100 nm (Aliyu et al., 2017; de Oliveira Carvalho et al., 2018; Deepika et al., 2020; Talavera et al., 2013).

3.1.4. EDS analysis

EDS is a method that uses X-ray energy to analyze the structure and chemical composition of samples on a small scale. Using the EDS analysis method, qualitative and quantitative analysis can be performed on a wide range of metallurgical, biological, mineral and ceramic samples. Using the obtained information, it is possible to investigate the quantity and quality of specific phases and areas with homogeneous chemical composition. In other words, this method can be used for

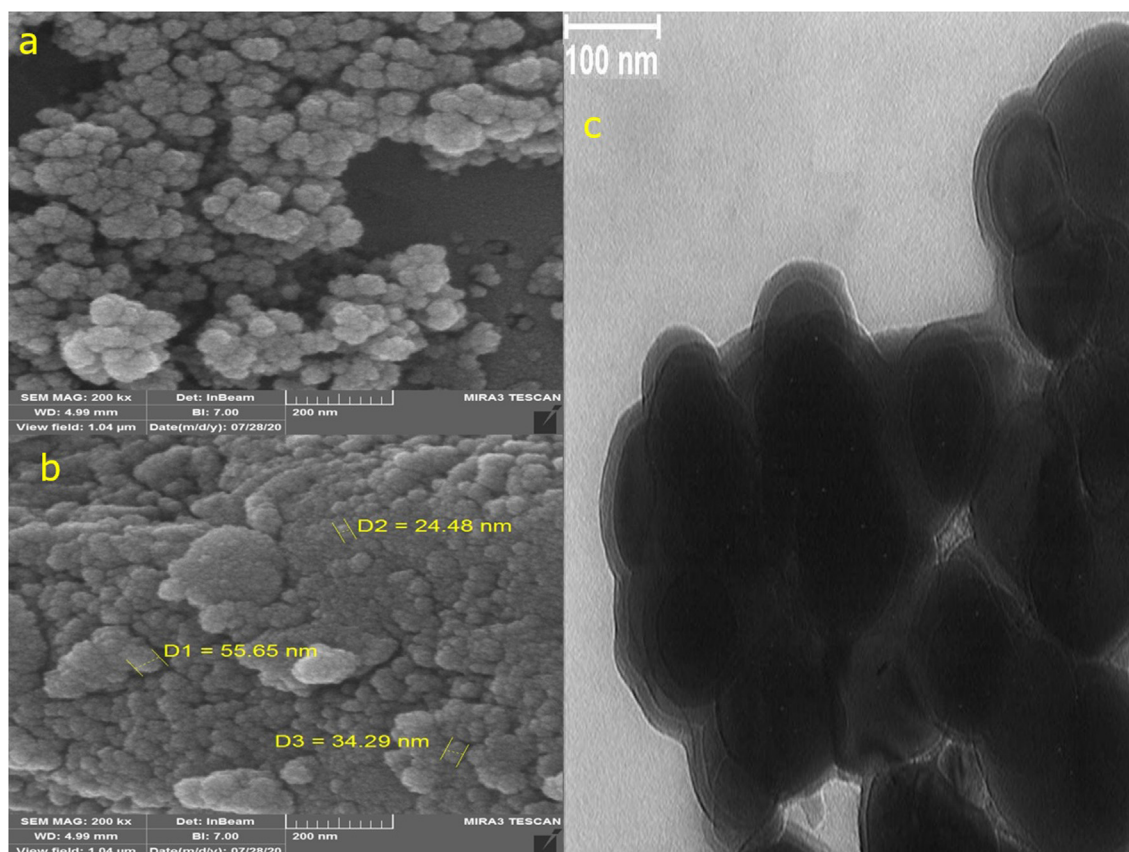


Fig. 3 a, b: SEM Images; c: TEM image of VNPs@*C.officinalis*.

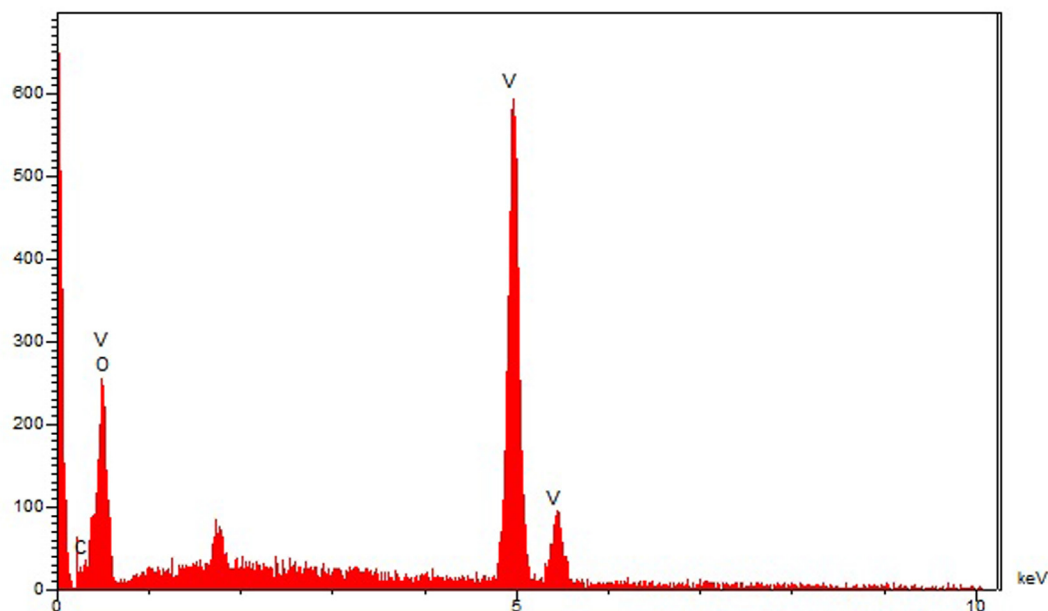


Fig. 4 EDS analysis of VNPs@*C.officinalis*.

microanalysis (Deepika et al., 2020). In EDS analysis, by measuring the energy of the emitted rays, we can identify the type of element under study, which is a method of qualitative analysis. By measuring the intensity of X-rays, the concentration of sample elements can be determined, making it possible to quantitatively analyze unknown samples. The higher the observed ipak for the element in the graph, the higher the concentration of that element in the sample. Also, as the energy of the electron beam increases and the atomic weight of the elements decreases, more depth can be obtained from the sample information (Deepika et al., 2020).

The EDS analysis of the synthetic NPs, as a semi-quantitative technique to recognize the elements, is shown in Fig. 4. The diagram presents the elemental composition profile of the VNPs@*C.officinalis*. The presence of vanadium was confirmed by the signals below of 1Kev (for VL α), around 5 Kev (for VK α), and after 5 Kev (for VK β). These signals are as well as match to those of biosynthesized VNPs that was reported previously (Deepika et al., 2020). The single before 0.5 Kev belongs to oxygen. This signal can be attributed to the oxygen in vanadium oxide nanoparticles and to the organic molecules present in *C. officinalis* extract that linked to the surface of VNPs@*C.officinalis*. The presence of carbon on the surface of VNPs@*C.officinalis* was approved by around 0.3 Kev.

3.2. Therapeutic properties of vanadium nanoparticles

Free radicals are molecules that do not have a complete electron shell, which increases the chemical reaction relative to others. Free radicals are formed if you are exposed to tobacco smoke and radiation. In humans, the most important free radical is oxygen. When an oxygen molecule (O₂) is exposed to radiation, it removes an electron from the other molecules, destroying DNA and other molecules (Abdoli et al., 2020; Jalalvand et al., 2019). Some of these changes cause disease. Problems such as heart problems, muscle failure, diabetes

and cancer are all caused by these free radicals. Antioxidants act like a broom against free radicals, destroying free radicals and regenerating damaged cells. Laboratory evidence has shown that antioxidants can prevent cancer (Abdoli et al., 2020; Jalalvand et al., 2019).

Studies have shown that the antioxidant features of vanadium nanoparticles green synthesized by pharmaceutical herbs are more significant than other metal nanoparticles. So far considerable antioxidant activities of metallic nanoparticles green-synthesized by several pharmaceuticals herbs like *Gundeliatournefortii* L., *Allium noeanum* Reut. ex Regel, *Falcaria vulgaris*, *Thymus vulgaris*, and *Camellia sinensis* have been confirmed. Vanadium nanoparticles green-synthesized by pharmaceuticals herbs show noticeable antioxidant activities against free radicals formation in the living system. Vanadium nanoparticles green-synthesized-formulated have important redox activities and have a noticeable role in free radicals dismantle (Abdoli et al., 2020; Jalalvand et al., 2019).

In this study, we assessed the antioxidant properties of *Calendula officinalis* leaf aqueous extract green-synthesized vanadium nanoparticles by using the DPPH test. The assay is used to evaluate the free radical scavenging activities of different antioxidant materials. This approach depends on the reduction of free radical DPPH by antioxidants in the absence of other free radicals, this action generates a color that absorption intensity can be evaluated by spectroscopy. The highest light absorption of DPPH radical at 515–520 nm in which methanolic solution is purple and acts as an electron absorber of a donor molecule like an antioxidant, thus changing DPPH to DPPH₂. Consequently, the purple color of the solution becomes yellow, therefore the absorption intensity decreases at 515–520 nm (Shaneza 'Aman et al., 2018).

We can find out the importance of antioxidant activities by evaluating the absorption intensity reduction through spectroscopy. The scavenging capacity of *Calendula officinalis* leaf aqueous extract green-synthesized vanadium nanoparticles

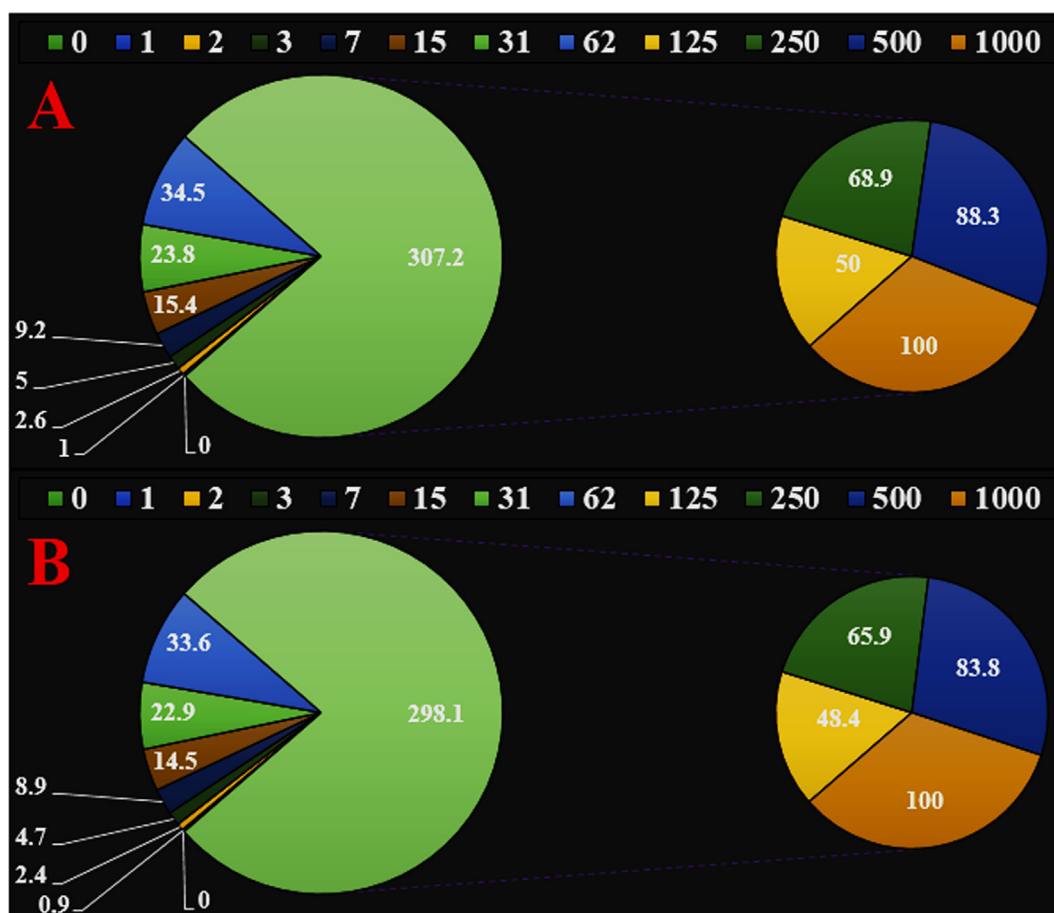


Fig. 5 The antioxidant properties of vanadium nanoparticles (A) and BHT (B) against DPPH. The numbers indicate the percent of free radical (DPPH) inhibition in the concentrations of 0–1000 µg/mL of vanadium nanoparticles and BHT.

Table 1 The IC₅₀ of vanadium nanoparticles and BHT in the antioxidant test.

	Vanadium nanoparticles	BHT
IC ₅₀ (µg/mL)	125	134

and BHT at different concentrations expressed as percentage inhibition has been indicated in Fig. 5.

Oxidation from reactive oxygen species can cause cell membrane disintegration, damage to membrane proteins, and DNA mutation that result is the onset or exacerbation of many diseases such as cancer, liver damage, and cardiovascular disease. Although the body has a defense system, constant exposure to chemicals and contaminants can lead to an increase in the number of free radicals outside the body's defense capacity and irreversible oxidative damage (Shaneza 'Aman et al., 2018). Therefore, antioxidants with the property of removing free radicals play an important role in the prevention or treatment of oxidation-related diseases or free radicals. Extensive molecular cell research on cancer cells has developed a targeted approach to the biochemical prevention of cancers that the goal is to stop or return cells to their pre-cancerous state without any toxic doses through nutrients and drugs (Abdoli et al.,

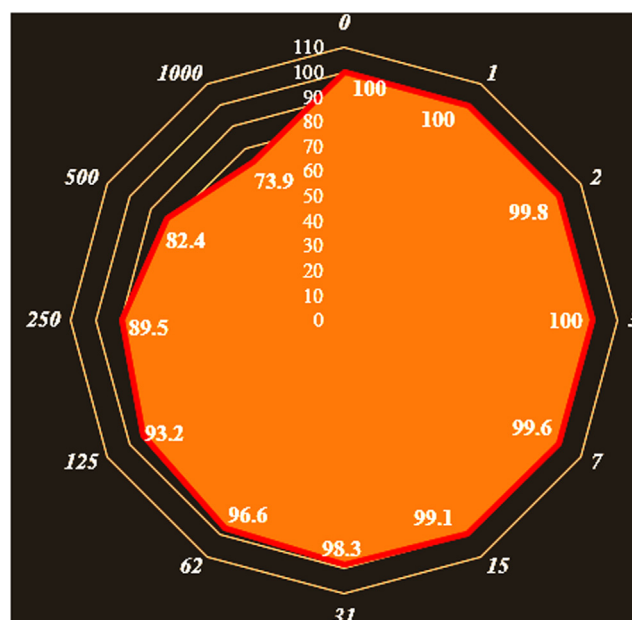


Fig. 6 The cell viability of vanadium nanoparticles against normal (HUVEC) cell line.

2020; Jalalvand et al., 2019). Numerous studies have been performed on using natural compounds as anti-cancer agents in relation to appropriate antioxidant activity (Shaneza 'Aman et al., 2018). It seems the high anti-cervical malignancy properties of the recent vanadium nanoparticles are related to its antioxidant compounds in the *Calendula officinalis* leaf aqueous extract. *Calendula officinalis* contain triterpenoid esters and the carotenoids flavoxanthin and auroxanthin (antioxidants and the source of the yellow-orange coloration) (Jalalvand et al., 2019). The leaves contain other carotenoids, mostly lutein (80%), zeaxanthin (5%), and beta-carotene. Plant extracts are also widely used by cosmetics, presumably due to the presence of compounds such as saponins, resins, and essential oils (Jalalvand et al., 2019).

In the antioxidant test, the IC₅₀ of vanadium nanoparticles and BHT were 144 and 201 µg/mL, respectively (Table 1).

In the cellular part of the study (Toxicological part), the treated cells with different concentrations of the present vanadium nanoparticles were assessed by MTT assay for 48 h about the cytotoxicity properties on normal (HUVEC) and cervical malignancy cell lines i.e. C-33 A [c-33a], SiHa, Ca Ski, DoTc2 4510, HT-3, and LM-MEL-41. The absorbance rate was evaluated at 570 nm, representing viability on normal cell line (HUVEC) even up to 1000 µg/mL for vanadium nanoparticles (Fig. 6).

The viability of malignant cervical cell line reduced dose-dependently in the presence of vanadium nanoparticles. The IC₅₀ of vanadium nanoparticles were 237, 259, 226, 409,

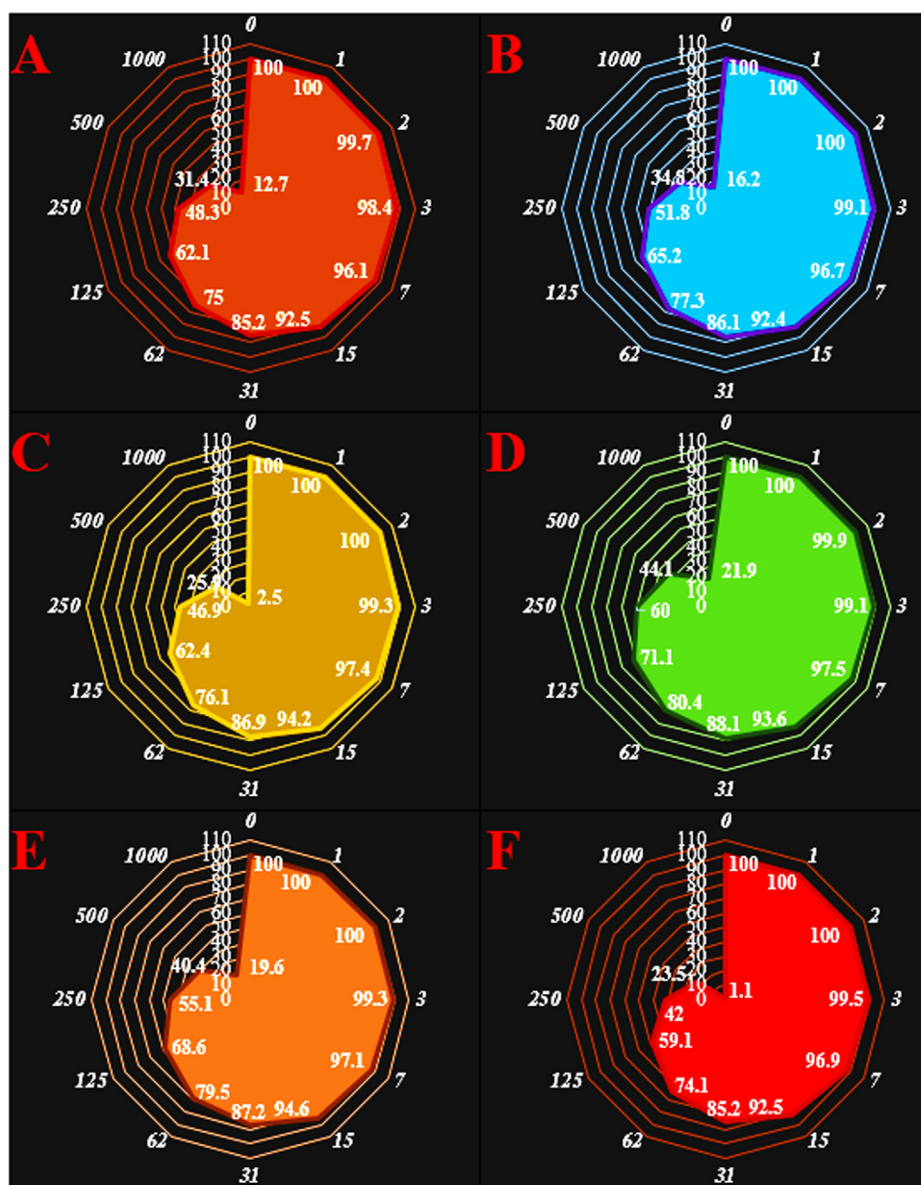


Fig. 7 The anti-human cervical cancer properties (Cell viability (%)) of vanadium nanoparticles (Concentrations of 0–1000 µg/mL) against common human cervical cancer cell lines i.e. C-33 A [c-33a] (A), SiHa (B), Ca Ski (C), DoTc2 4510 (D), HT-3 (E), and LM-MEL-41 (F).

Table 2 The IC₅₀ of vanadium nanoparticles in the anti-human cervical cancer test.

	HUVEC	C-33 A [c-33a]	SiHa	Ca Ski	DoTc2 4510	HT-3	LM-MEL-41
IC ₅₀ (μg/mL)	–	237	259	226	409	335	192

335, and 192 μg/mL against C-33 A [c-33a], SiHa, Ca Ski, DoTc2 4510, HT-3, and LM-MEL-41 cell lines, respectively (Fig. 7 and Table 2).

The numbers indicate the percent of cell viability in the concentrations of 0–1000 μg/mL of vanadium nanoparticles against several cervical cancer cell lines.

Metallic nanoparticles have various parameters such as shape, size, texture, etc. Sizes have very significant properties in the therapeutic effects of nanoparticles, some studies reported that small metallic nanoparticles have better entrance into cells and have significant anti-cancer activities. It has been assessed that particle size lower than 50 nm showed an excellent remedial feature in the corresponding cancer cell lines (Mao et al., 2016; Namvar et al., 2014; Sankar et al., 2014; Tahvilian et al., 2019; You et al., 2012). As you see in Figure of FE-SEM of our study, the average size of vanadium nanoparticles synthesized by *Calendula officinalis* leaf aqueous extract is less than 50 nm. Metallic nanoparticles have been utilized to treat various cancers including Lewis lung carcinoma, human glioma, human lung cancer, uterus cancer, lung epithelial cancer, colon cancer, and mammary carcinoma (Abdoli et al., 2020; Jalalvand et al., 2019).

Maybe important anti-human cervical cancer potentials of vanadium nanoparticles synthesized by *Calendula officinalis* leaf aqueous extract against malignant cervical cell lines i.e., C-33 A [c-33a], SiHa, Ca Ski, DoTc2 4510, HT-3, and LM-MEL-41 due to their antioxidant activities. Corresponding reports have indicated the antioxidant materials like pharmaceuticals plants and metallic nanoparticles especially vanadium nanoparticles reduce the volume of tumors by scavenging free radicals (Katata-Seru et al., 2018). Generally, the presence of free radicals in the body causes countless chain reactions in the body that gives rise to the production of more free radicals, also causes a variety of mutations in the structure of DNA and RNA, and cause an uncontrolled increase in malignant cell proliferation and finally damage the body (Beheshtkhoo et al., 2018; Sangami and Manu, 2017). The high concentration of free radicals present in all kinds of cancer, free radicals causes tumorigenesis and angiogenesis (Beheshtkhoo et al., 2018; Katata-Seru et al., 2018; Sangami and Manu, 2017).

Many studies worldwide have reported that vanadium nanoparticles synthesized by pharmaceuticals plants have a significant role in eliminating free radicals and are involved in preventing the growth of malignant cells (Oganesvan et al., 1991; Radini et al., 2018).

4. Conclusion

The vanadium nanoparticles showed the best antioxidant activities against DPPH. Vanadium nanoparticles had appropriate anti-human cervical cancer activities dose-dependently against C-33 A [c-33a], SiHa, Ca Ski, DoTc2 4510, HT-3, and LM-MEL-41 cell lines without any cytotoxicity on the

normal cell line (HUVEC). The IC₅₀ of vanadium nanoparticles were 237, 259, 226, 409, 335, and 192 μg/mL against C-33 A [c-33a], SiHa, Ca Ski, DoTc2 4510, HT-3, and LM-MEL-41 cell lines, respectively. After clinical study vanadium nanoparticles containing *Calendula officinalis* leaf, aqueous extract can be utilized as an efficient drug in treating cervical cancer in humans.

Declaration of Competing Interest

None.

Acknowledgment

Authors extend their appreciation to the Deanship of Scientific Research at King Saud University for funding this work through research group no (RG-1435-065).

References

- Abdoli, M., Sadrajavadi, K., Arkan, E., Zangeneh, M.M., Moradi, S., Zangeneh, A., Shahlaei, M., Khaledian, S., 2020. Polyvinyl alcohol/Gum tragacanth/graphene oxide composite nanofiber for antibiotic delivery. *J. Drug Deliv. Sci. Technol.* 60, 102044.
- Ahmeda, A., Zangeneh, A., Zangeneh, M.M., 2020. Green synthesis and chemical characterization of gold nanoparticle synthesized using *Camellia sinensis* leaf aqueous extract for the treatment of acute myeloid leukemia in comparison to daunorubicin in a leukemic mouse model. *Appl. Organomet. Chem.* 34, e5290.
- Aliyu, A., Garba, S., Bognet, O., 2017. Green synthesis, characterization and antimicrobial activity of vanadium nanoparticles using leaf extract of *Moringa Oleifera*. *Int. J. Chem. Sc.* 16, 231.
- Arunachalam, K.D., Annamalai, S.K., Hari, S., 2013. One-step green synthesis and characterization of leaf extract-mediated biocompatible silver and gold nanoparticles from *Memecylon umbellatum*. *Int. J. Nanomed.* 8, 1307.
- Baghayeri, M., Mahdavi, B., Hosseinpor-Mohsen Abadi, Z., Farhadi, S., 2018. Green synthesis of silver nanoparticles using water extract of *Salvia leriifolia*: Antibacterial studies and applications as catalysts in the electrochemical detection of nitrite. *Appl. Organomet. Chem.* 32, e4057.
- Beheshtkhoo, N., Kouhbanani, M.A.J., Savardashtaki, A., Amani, A. M., Taghizadeh, S., 2018. Green synthesis of iron oxide nanoparticles by aqueous leaf extract of *Daphne mezereum* as a novel dye removing material. *Appl. Phys. A* 124, 363.
- Burke, W.M., Orr, J., Leitao, M., Salom, E., Gehrig, P., Olawaiye, A. B., Brewer, M., Boruta, D., Herzog, T.J., Shahin, F.A., 2014. Endometrial cancer: a review and current management strategies: part II. *Gynecol. Oncol.* 134, 393–402.
- Clarke, M.A., Long, B.J., Morillo, A.D.M., Arbyn, M., Bakkum-Gomez, J.N., Wentzensen, N., 2018. Association of endometrial cancer risk with postmenopausal bleeding in women: a systematic review and meta-analysis. *JAMA Internal Med.* 178, 1210–1222.
- de Oliveira Carvalho, H., Góes, L.D.M., Cunha, N.M.B., Ferreira, A. M., Fernandes, C.P., Favacho, H.A.S., Junior, J.O.C.S., Ortiz, B. L.S., Navarrete, A., Carvalho, J.C.T., 2018. Development and

- standardization of capsules and tablets containing *Calendula officinalis* L. hydroethanolic extract. *Revista Latinoamericana de Química* 46, 16–27.
- Deepika, P., Vinusha, H., Muneera, B., Rekha, N., Prasad, K.S., 2020. Vanadium oxide nanorods as DNA cleaving and anti-angiogenic agent: Novel green synthetic approach using leaf extract of *Tinospora cordifolia*. *Curr. Res. Green Sustain. Chem.*
- Długosz, M., Markowski, M., Pączkowski, C., 2018. Source of nitrogen as a factor limiting saponin production by hairy root and suspension cultures of *Calendula officinalis* L. *Acta Physiologica Plantarum* 40, 35.
- Fahimmunisha, B.A., Ishwarya, R., AlSalhi, M.S., Devanesan, S., Govindarajan, M., Vaseeharan, B., 2020. Green fabrication, characterization and antibacterial potential of zinc oxide nanoparticles using *Aloe socotrina* leaf extract: A novel drug delivery approach. *J. Drug Deliv. Sci. Technol.* 55, 101465.
- Ghashghaai, A., Hashemnia, M., Nikousefat, Z., Zangeneh, M.M., Zangeneh, A., 2017. Wound healing potential of methanolic extract of *Scrophularia striata* in rats. *Pharmaceut. Sci.* 23, 256–263.
- Ghidan, A.Y., Al-Antary, T.M., Awwad, A.M., 2016. Green synthesis of copper oxide nanoparticles using *Punica granatum* peels extract: Effect on green peach Aphid. *Environ. Nanotechnol. Monit. Manage.* 6, 95–98.
- Goorani, S., Shariatfar, N., Seydi, N., Zangeneh, A., Moradi, R., Tari, B., Nazari, F., Zangeneh, M.M., 2019. The aqueous extract of *Allium saralicum* RM Fritsch effectively treat induced anemia: experimental study on Wistar rats. *Oriental Pharm. Exp. Med.* 19, 403–413.
- Guillot, D., Martin, S.A., 2014. Exploiting DNA mismatch repair deficiency as a therapeutic strategy. *Exp. Cell Res.* 329, 110–115.
- Jalalvand, A.R., Zhaleh, M., Goorani, S., Zangeneh, M.M., Seydi, N., Zangeneh, A., Moradi, R., 2019. Chemical characterization and antioxidant, cytotoxic, antibacterial, and antifungal properties of ethanolic extract of *Allium Saralicum* RM Fritsch leaves rich in linolenic acid, methyl ester. *J. Photochem. Photobiol., B* 192, 103–112.
- Kang, W., Yan, C., Wang, X., Foo, C.Y., Tan, A.W.M., Chee, K.J.Z., Lee, P.S., 2014. Green synthesis of nanobelt-membrane hybrid structured vanadium oxide with high electrochromic contrast. *J. Mater. Chem. C* 2, 4727–4732.
- Karthik, K., Nikolova, M.P., Phuruangrat, A., Pushpa, S., Revathi, V., Subbulakshmi, M., 2020. Ultrasound-assisted synthesis of V₂O₅ nanoparticles for photocatalytic and antibacterial studies. *Mater. Res. Innovat.* 24, 229–234.
- Katata-Seru, L., Moremedi, T., Aremu, O.S., Bahadur, I., 2018. Green synthesis of iron nanoparticles using *Moringa oleifera* extracts and their applications: removal of nitrate from water and antibacterial activity against *Escherichia coli*. *J. Mol. Liq.* 256, 296–304.
- Khan, Z.U.H., Sadiq, H.M., Shah, N.S., Khan, A.U., Muhammad, N., Hassan, S.U., Tahir, K., Khan, F.U., Imran, M., Ahmad, N., 2019. Greener synthesis of zinc oxide nanoparticles using *Trianthema portulacastrum* extract and evaluation of its photocatalytic and biological applications. *J. Photochem. Photobiol., B* 192, 147–157.
- Mahdavi, B., Paydarfard, S., Zangeneh, M.M., Goorani, S., Seydi, N., Zangeneh, A., 2020. Assessment of antioxidant, cytotoxicity, antibacterial, antifungal, and cutaneous wound healing activities of green synthesized manganese nanoparticles using *Ziziphora clinopodioides* Lam leaves under in vitro and in vivo condition. *Appl. Organomet. Chem.* 34, e5248.
- Mahdavi, B., Saneci, S., Qorbani, M., Zhaleh, M., Zangeneh, A., Zangeneh, M.M., Pirabbasi, E., Abbasi, N., Ghaneialvar, H., 2019. *Ziziphora clinopodioides* Lam leaves aqueous extract mediated synthesis of zinc nanoparticles and their antibacterial, antifungal, cytotoxicity, antioxidant, and cutaneous wound healing properties under in vitro and in vivo conditions. *Appl. Organomet. Chem.* 33, e5164.
- Mao, B.-H., Tsai, J.-C., Chen, C.-W., Yan, S.-J., Wang, Y.-J., 2016. Mechanisms of silver nanoparticle-induced toxicity and important role of autophagy. *Nanotoxicology* 10, 1021–1040.
- Moradi, R., Hajjalilani, M., Salmani, S., Almasi, M., Zangeneh, A., Zangeneh, M.M., 2019. Effect of aqueous extract of *Allium saralicum* RM Fritsch on fatty liver induced by high-fat diet in Wistar rats. *Comp. Clin. Pathol.* 28, 1205–1211.
- Murali, R., Soslow, R.A., Weigelt, B., 2014. Classification of endometrial carcinoma: more than two types. *Lancet Oncol.* 15, e268–e278.
- Namvar, F., Rahman, H.S., Mohamad, R., Baharara, J., Mahdavi, M., Amini, E., Chartrand, M.S., Yeap, S.K., 2014. Cytotoxic effect of magnetic iron oxide nanoparticles synthesized via seaweed aqueous extract. *Int. J. Nanomed.* 9, 2479.
- Oganesvan, G., Galstyan, A., Mnatsakanyan, V., Paronikyan, R., Ter-Zakharyan, Y.Z., 1991. Phenolic and flavonoid compounds of *Ziziphora clinopodioides*. *Chem. Nat. Compd.* 27, 247–247.
- Prasad, K.S., Shivamallu, C., Shruthi, G., Prasad, M., 2018. A Novel and One-pot Green Synthesis of Vanadium Oxide Nanorods Using a Phytomolecule Isolated from *Phyllanthus amarus*. *ChemistrySelect* 3, 3860–3865.
- Radini, I.A., Hasan, N., Malik, M.A., Khan, Z., 2018. Biosynthesis of iron nanoparticles using *Trigonella foenum-graecum* seed extract for photocatalytic methyl orange dye degradation and antibacterial applications. *J. Photochem. Photobiol., B* 183, 154–163.
- Rashidi, K., Mahmoudi, M., Mohammadi, G., Zangeneh, M.M., Korani, S., Goicoechea, H.C., Gu, H.-W., Jalalvand, A.R., 2018. Simultaneous co-immobilization of three enzymes onto a modified glassy carbon electrode to fabricate a high-performance amperometric biosensor for determination of total cholesterol. *Int. J. Biol. Macromol.* 120, 587–595.
- Raut, R.W., Kolekar, N.S., Lakkakula, J.R., Mendhulkar, V.D., Kashid, S.B., 2010. Extracellular synthesis of silver nanoparticles using dried leaves of *Pongamia pinnata* (L) pierre. *Nano-Micro Lett.* 2, 106–113.
- Sangami, S., Manu, B., 2017. Synthesis of Green Iron Nanoparticles using Laterite and their application as a Fenton-like catalyst for the degradation of herbicide Ametryn in water. *Environ. Technol. Innovation* 8, 150–163.
- Sankar, R., Maheswari, R., Karthik, S., Shivashangari, K.S., Ravikumar, V., 2014. Anticancer activity of *Ficus religiosa* engineered copper oxide nanoparticles. *Mater. Sci. Eng., C* 44, 234–239.
- Seydi, N., Mahdavi, B., Paydarfard, S., Zangeneh, A., Zangeneh, M. M., Najafi, F., Jalalvand, A.R., Pirabbasi, E., 2019. Preparation, characterization, and assessment of cytotoxicity, antioxidant, antibacterial, antifungal, and cutaneous wound healing properties of titanium nanoparticles using aqueous extract of *Ziziphora clinopodioides* Lam leaves. *Appl. Organomet. Chem.* 33, e5009.
- Shaneza Aman, Umesh Kumar Gupta, Deepa Singh, Khan, T., 2018. Herbal treatment for the ovarian cancer. *SGVU J. Pharmaceut. Res. Educ.*, vol. 3, 325–329.
- Sherkatolabbasieh, H., Hagh-Nazari, L., Shafieezadeh, S., Goodarzi, N., Zangeneh, M.M., Zangeneh, A., 2017. Ameliorative effects of the ethanolic extract of *Allium saralicum* RM Fritsch on CCl₄-induced nephrotoxicity in mice: a stereological examination. *Arch. Biol. Sci.* 69, 535–543.
- Sintubin, L., De Windt, W., Dick, J., Mast, J., Van Der Ha, D., Verstraete, W., Boon, N., 2009. Lactic acid bacteria as reducing and capping agent for the fast and efficient production of silver nanoparticles. *Appl. Microbiol. Biotechnol.* 84, 741–749.
- Tahvilian, R., Zangeneh, M.M., Falahi, H., Sadrjavadi, K., Jalalvand, A.R., Zangeneh, A., 2019. Green synthesis and chemical characterization of copper nanoparticles using *Allium saralicum* leaves and assessment of their cytotoxicity, antioxidant, antimicrobial, and cutaneous wound healing properties. *Appl. Organomet. Chem.* 33, e5234.

- Talavera, N., Navarro, M., Sifontes, A., Díaz, Y., Villalobos, H., Niño-Vega, G., Boada-Sucre, A., González, I., 2013. Green synthesis of nanosized vanadium pentoxide using *Saccharomyces cerevisiae* as biotemplate. *Recent Res. Develop. Mater. Sci.* 10, 89.
- Verma, P.K., Raina, R., Agarwal, S., Kaur, H., 2018. Phytochemical ingredients and Pharmacological potential of *Calendula officinalis* Linn. *Pharmaceut. Biomed. Res.* 4, 1–17.
- You, C., Han, C., Wang, X., Zheng, Y., Li, Q., Hu, X., Sun, H., 2012. The progress of silver nanoparticles in the antibacterial mechanism, clinical application and cytotoxicity. *Mol. Biol. Rep.* 39, 9193–9201.